Effects of AIF Variations on DCE-MRI Prediction of Breast Cancer Therapy Response

Aneela Afzal[1], Alina Tudorica[1], Yiyi Chen[1], Stephen Y-C Chui[1], Arpana Naik[1], Megan L Troxell[1], Kathleen A Kemmer[1], Karen Y Oh[1], Nicole Roy[1], Megan L Holtorf[1], Xin Li[1], and Wei Huang[1]

[1]*Oregon Health & Science University, Portland, OR, United States*

Introduction: As a functional imaging method for characterizing tissue microvasculature, dynamic contrast-enhanced MRI (DCE-MRI) is increasingly used in research settings and early phase clinical trials to assess tumor therapeutic response (1,2). Pharmacokinetic (PK) analysis of DCE-MRI data is often used to obtain quantitative biological parameters, such as K^{trans} and v_e. However, the accuracy and precision of these parameters can be affected by many factors in data acquisition and analysis, one of which is the determination of arterial input function (AIF) (2-4). A recent study (5) shows that two different AIF quantification approaches, individually measured AIF and cohort-based average AIF, can result in substantial variations in prostate tumor PK parameters. However, little has been reported on whether AIF-caused variations in PK parameters affect the effectiveness of DCE-MRI as an imaging tool to evaluate cancer response to therapy. In this study of retrospective analysis of breast DCE-MRI data, we sought to examine the effects of different AIF methods on DCE-MRI prediction of breast cancer response to neoadjuvant chemotherapy (NACT).

Table 1. DCE-MRI Metrics Estimated with Different AIF methods

AIF	V1			V2			V21 (%)		
	K^{trans} (min^{-1})	v_e	τ_i (s)	K^{trans} (min^{-1})	v_e	τ_i (s)	K^{trans}	v_e	τ_i
<AIF>	0.071 ± 0.033*#	0.24 ± 0.09*#	0.60 ± 0.22	0.053 ± 0.030*#	0.34 ± 0.17*#	0.70 ± 0.22	-33 ± 53	64 ± 88	16 ± 59
$<AIF>_R$	0.11 ± 0.07	0.35 ± 0.18	0.66 ± 0.24	0.10 ± 0.08	0.51 ± 0.22	0.69 ± 0.22	-23 ± 74	82 ± 95	14 ± 64
$<AIF>_{P,R}$	0.11 ± 0.07	0.38 ± 0.20	0.62 ± 0.23	0.11 ± 0.10	0.52 ± 0.24	0.67 ± 0.29	-18 ± 81	88 ± 85	14 ± 68

Paired t test: *, $P < 0.05$, <AIF> against $<AIF>_R$; #, $P < 0.05$, <AIF> against $<AIF>_{P,R}$

Methods: Research DCE-MRI data were collected with consent from 29 consecutive patients with locally advanced breast cancer who underwent NACT before definitive surgery. The MRI studies were performed at visit 1 (V1, before NACT), V2 (after 1 NACT cycle), V3 (at NACT midpoint – usually between third and fourth cycles), and V4 (after NACT, before surgery). Axial bilateral DCE-MRI images were acquired with a 3D GRE-based TWIST sequence (6) using a 3T Siemens scanner. An image volume of 120-128 slices (for full breast coverage) was acquired 32-34 times with 18-20 s temporal resolution for a total duration of ~ 10 min. Tumor ROIs on multiple slices were drawn by experienced radiologists. DCE-MRI time-course data from voxels within the ROIs were then subjected to PK analyses using the Shutter-Speed model (SSM) that takes into account transcytolemmal water exchange kinetics (7). The whole tumor mean PK parameter values were calculated, which included K^{trans}, v_e, and the SSM-unique τ_i parameter, the mean intracellular water lifetime.

Three AIF quantification approaches were used for PK analysis of each DCE-MRI data set. The first AIF, <AIF>, was an average of three individually measured AIFs from an axillary artery in another breast DCE-MRI study (8) with higher temporal resolution but the same IV contrast injection protocol (dose, injection rate and site) as this study. The second AIF, $<AIF>_R$, was the same as <AIF>, except that the <AIF> amplitude was adjusted using a chest wall muscle ROI as the reference region. For each study, the $<AIF>_R$ peak height was adjusted until PK analysis of the muscle ROI data using $<AIF>_R$ and Tofts model returned a literature v_e value of 0.1 (9). The third AIF, $<AIF>_{P,R}$, was the population-averaged AIF published by Parker *et al.* (10) with its amplitude adjusted in the same fashion as the $<AIF>_R$ for each study.

In this preliminary analysis, only the effects of AIF variation on DCE-MRI early prediction of therapy response were investigated. Therefore, only the PK parameters at V1 and V2, and their percent changes (V21%, V2 relative to V1) obtained with the three AIF methods were compared for predictive ability. Paired t test was used to assess AIF-caused parameter variations. Correlating with pathologic response endpoints, Receiver Operating Characteristic (ROC) analysis was used to evaluate accuracies of the MRI metrics for early prediction of response. A nonparametric method was used to compare ROC area-under-the-curve (AUC) among the three AIF approaches.

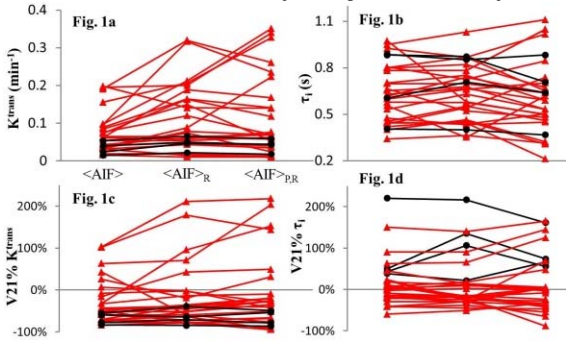

Results: Pathology analysis of post-NACT resection specimens revealed that four patients had pathologic complete response (pCR), while the other 25 patients were non-pCRs. **Table 1** lists the tumor mean ± SD values of K^{trans}, v_e, and τ_i at V1, V2, and V21% obtained with the three AIF approaches for the entire 29-patient cohort. The paired t test showed that the estimated K^{trans} and v_e values at V1 or V2 were significantly ($P < 0.05$) different when comparing <AIF> against $<AIF>_R$ or $<AIF>_{P,R}$. However, this was not the case for comparison of $<AIF>_R$ against $<AIF>_{P,R}$. There was no significant difference in the estimated τ_i value when comparing any two AIF methods, neither were there in V21% values of all three parameters. Illustrating a few examples, **Fig. 1** shows scatter plots of V2 K^{trans} (1a), V2 τ_i (1b), V21% K^{trans} (1c), and V21% τ_i (1d) with black circles representing pCRs and red triangles non-pCRs. The straight line connects data points obtained with the three AIF methods (labeled in Fig. 1a) from the same tumor.

We have previously shown that V2 K^{trans}, V21% K^{trans}, and V21% τ_i estimated using the <AIF> method are good early predictors of breast cancer response to NACT (11). **Table 2** lists the ROC AUC values for these three metrics under the condition of three different AIF approaches, indicating that these three metrics remain good early predictors of therapy response regardless of the AIF chosen for PK analysis. For each metric there was no statistically significant difference in ROC AUC among the three AIF methods.

Table 2. Early Prediction of Response

MRI Metrics	ROC AUC		
	<AIF>	$<AIF>_R$	$<AIF>_{P,R}$
V2 K^{trans}	0.76	0.72	0.70
V21% K^{trans}	0.79	0.76	0.77
V21% τ_i	0.89	0.95	0.88

Discussion and Conclusion: The results from this study suggest that AIF amplitude may be the dominant factor affecting the estimated PK parameter values. Despite substantial difference in the shape of $<AIF>_R$ and $<AIF>_{P,R}$ – empirical expression (8) for the former and a mixture of two Gaussian kernels plus an exponential (10) for the latter, the estimated PK parameters are not significantly different between the two AIFs after the peak heights of both were adjusted using a normal muscle region as reference. On the other hand, the AIF-caused PK parameter variations observed here are most likely systematic, resulting in non-significant difference in parameter V21% value between any two AIFs. This is possibly also the reason why V2 K^{trans} and V21% K^{trans} remain good early predictors of therapy response irrespective of the AIF used. The τ_i value was not significantly altered by AIF selection, which is in agreement with a recent simulation study (12). Not surprisingly, V21% τ_i remains a good metric for early prediction of breast cancer therapy response with any of the three AIF methods. For a multicenter trial of DCE-MRI evaluation of tumor therapy response, it may be a sound approach to use a normal tissue area as a reference region to adjust the peak height of measured AIF in each center. This could minimize PK parameter variations and lead to more consistent results in therapeutic monitoring across centers.

Grant Support: NIH U01 CA154602.

References: **1.** O'Connor *et al. Nat Rev Clin Oncol* 2012;9:167-77. **2.** Leach *et al. Eur Radiol* 2012;22:1451-64. **3.** Yankeelov *et al. Curr Med Imaging Rev* 2009;3:91-107. **4.** Sourbron *et al. Phys Med Biol* 2012;57:R1-R33. **5.** Fedorov *et al. Magn Reson Imaging* 2014;32:321-9. **6.** Tudorica *et al. Magn Reson Imaging* 2012;30:1257-1267. **7.** Yankeelov *et al. Magn Reson Med* 2003;50:1151-1169. **8.** Huang *et al. Radiology* 2011;261:394-403. **9.** Li *et al. JMR* 2010;206:190-9. **10.** Parker *et al. Magn Reson Med* 2006;56:993-1000. **11.** Tudorica *et al. Proc Intl Soc Magn Reson Med* 2014;22:920. **12.** Li X *et al. Proc Intl Soc Magn Reson Med* 2014;22:4595.